Faceted patterns and anomalous surface roughening driven by long-range temporally correlated noise

Alejandro Alés[1] and Juan M. López[2,*]

[1]*Instituto de Investigaciones Físicas de Mar del Plata (IFIMAR), Facultad de Ciencias Exactas y Naturales, Universidad Nacional de Mar del Plata, Consejo Nacional de Investigaciones Científicas y Técnicas (CONICET), Deán Funes 3350, B7602AYL Mar del Plata, Argentina*

[2]*Instituto de Física de Cantabria (IFCA), CSIC–Universidad de Cantabria, 39005 Santander, Spain*

(Received 14 February 2019; revised manuscript received 23 April 2019; published 28 June 2019)

We investigate Kardar-Parisi-Zhang (KPZ) surface growth in the presence of power-law temporally correlated noise. By means of extensive numerical simulations of models in the KPZ universality class we find that, as the noise correlator index increases above some threshold value, the surface exhibits anomalous kinetic roughening of the type described by the generic scaling theory of Ramasco *et al.* [Phys. Rev. Lett. **84**, 2199 (2000)]. Remarkably, as the driving noise temporal correlations increase, the surface develops a characteristic pattern of macroscopic facets that completely dominates the dynamics in the long time limit. We argue that standard scaling fails to capture the behavior of KPZ subject to long-range temporally correlated noise. These phenomena are not not described by the existing theoretical approaches, including renormalization group and self-consistent approaches.

DOI: 10.1103/PhysRevE.99.062139

I. INTRODUCTION

The dynamics of surfaces and interfaces driven by random fluctuations has many applications in modern condensed matter science and statistical physics, including the description of surfaces formed by particle deposition processes in thin-film growth (e.g., molecular-beam epitaxy, sputtering, electrodeposition, and chemical-vapor deposition) [1,2], advancing fracture cracks in disordered materials [3], and fluid-flow depinning in disordered media [4]. The dynamics of scale-invariant interfaces is also relevant to understand many classical problems in statistical mechanics, including directed polymers in random media, minimal energy paths, and localization in disordered media [5,6]. Remarkably, it has also been found recently that there exists a deep connection of interface kinetic roughening with the evolution of perturbations, the so-called Lyapunov vectors, in chaotic spatially extended dynamical systems [7–14]. All these theoretical interconnections between apparently distant problems make the understanding of all aspects of kinetic surface roughening a central theme in modern statistical physics.

The time-evolution, Langevin-type equation for the surface height $h(\mathbf{x},t)$ in most of the above mentioned systems satisfies a set of fundamental symmetries (rotational, translational in $\mathbf{x}$, time invariance, etc.), including the fundamental *shift* symmetry $h \to h + c$, where c is a constant [1]. The latter immediately leads to scale-invariant surfaces or interfaces without fine tuning of any external parameters or couplings, which implies generic power-law decay of the spatiotemporal surface height correlations [15]. In a nutshell, a surface is said to be scale invariant if its statistical properties remain unchanged after rescaling of space and time according to the transformation $h(\mathbf{x},t) \to b^{\alpha} h(b\,\mathbf{x}, b^{1/z}\,t)$, for any scaling factor $b > 1$ and a certain combination of critical exponents α and z [1,2].

In kinetic surface roughening the Kardar-Parisi-Zhang (KPZ) [16] equation plays a central role as the simplest, nonlinear, out-of-equilibrium model in the continuum exhibiting scale-invariant solutions. The KPZ model represents a universality class of surface growth that brings together many different surface dynamics that share the same symmetries including Eden growth, ballistic deposition, and Kim-Kosterlitz growth models among many others [1,2]. The KPZ equation describes the evolution of the interface height $h(\mathbf{x},t)$ at time t and substrate position $\mathbf{x}$ in $d+1$ dimensions and is given by [16]

$$\partial_t h(\mathbf{x},t) = \nu \nabla^2 h + \lambda (\nabla h)^2 + \eta(\mathbf{x},t), \tag{1}$$

where $\eta(\mathbf{x},t)$ is an uncorrelated noise

$$\langle \eta(\mathbf{x},t)\eta(\mathbf{x}',t')\rangle = 2D\delta(\mathbf{x}-\mathbf{x}')\delta(t-t'). \tag{2}$$

The KPZ equation with uncorrelated noise has scale-invariant solutions, as can be rigorously proven by calculating height-height correlation functions by means of dynamic renormalization group (RG) techniques [16]. In $1+1$ dimensions one can obtain the exact critical exponents $\alpha = 1/2$ and $z = 3/2$ almost straightforwardly (see for instance [1]) after realizing that, on the one hand, the stationary solution of the Fokker-Planck equation associated with the Langevin dynamics, Eq. (1), in $d = 1$ is identical to that of the linear ($\lambda = 0$) case, implying $\alpha = 1/2$, and, on the other hand, that Eq. (1) satisfies Galilean invariance (in any dimension), which implies the hyperscaling relation $\alpha + z = 2$. In contrast, exact exponents are not known in higher dimensions, due to the existence of a strong-coupling fixed point for $d > 1$ that cannot be approached with pertubative RG calculations, and have been estimated from numerical simulations [17–25] or analytical approximations of several sorts [26–29].

*lopez@ifca.unican.es

In many applications the noise is actually correlated. If correlations are short-ranged one expects that, in the long wavelength limit, the critical exponents should remain exactly the same as in the case of uncorrelated noise. Indeed, this result can be rigorously proven by, for instance, RG arguments. However, in systems where noise correlations are long-ranged the critical exponents do depend on the noise correlator decay exponents, as was early shown by Medina *et al.* [30] using perturbative RG.

While the effect of spatially correlated noise in KPZ has been extensively studied in the literature [31–45], the case of algebraic temporal correlations has remained virtually unexplored so far [46–49]. Interestingly, the effect of temporally correlated noise in kinetic roughening has earned renewed interest, as it has been very recently shown to play a crucial, and not yet completely understood, role in the interface picture of infinitesimal perturbations (Lyapunov vectors) [10,14,50] and the scaling of the Lyapunov exponent fluctuations in spatiotemporal chaos [8].

In this article we show that KPZ growth in the presence of temporally correlated noise gives rise to surfaces with a macroscopic faceted structure, i.e., the surface is formed by long flat faces. The origin of the faceted pattern and the accompanying anomalous kinetic roughening can be traced back to the strong localization properties of the field $\phi(\mathbf{x}, t) = \exp h(\mathbf{x}, t)$, and the same mechanism is expected to be relevant for other surface growth models. Our conclusions are based upon extensive numerical simulations of two models in the same universality class. We studied ballistic deposition as an example of a discrete growth model with KPZ symmetries. We also performed a direct numerical integration of the KPZ equation (1) with a long-range temporally correlated noise.

II. MODELS

A. Long-time correlated noise

In our numerical study we needed to generate very long time series of random numbers with long temporal correlations at every spatial position x. In particular, one must generate a spatially uncorrelated time series $\eta(x, t)$ at every lattice site x and be certain that the power spectrum $\langle|\hat{\eta}(x, \omega)|^2\rangle$, where $\langle\cdots\rangle$ denotes noise average, exhibits excellent scaling at low frequencies so that, at leading order, $\langle|\hat{\eta}(x, \omega)|^2\rangle \sim \omega^{-2\theta}$ for $\omega \to 0$ at every lattice site x, and the noise correlator scales as

$$\langle\eta(x, t)\eta(x', t')\rangle = 2D\,\delta_{x,x'}\,|t - t'|^{2\theta-1}, \tag{3}$$

for time differences $|t - t'| > L^z$. In this way, we can be certain that we have spatially uncorrelated noise with power-law scaling of the temporal correlations for times differences up to, at least, the saturation time in a system of size L. The exponent $\theta \in [0, 1/2)$ characterizes the temporal correlation range of the noise that becomes more long-term correlated as θ is increased from zero.

For each lattice site x we generated a noise sequence parameterized by t using the Mandelbrot's fast fractional Gaussian noise generator [51,52]. This algorithm produces a random sequence of Gaussian distributed numbers $Z(t)$ which can be used in the numerical integration of the KPZ equation, $\eta(x, t) \equiv Z_x(t)$, by generating L independent Mandelbrot sequences $Z_1(t), Z_2(t), \ldots, Z_L(t)$. In the case of the simulations of particle deposition by ballistic deposition, we map $\eta(x, t) = 1$ if $Z_x(t) > 0$ and $\eta(x, t) = 0$ otherwise. This *digitalization* of the noise enhances the statistics of the simulations by avoiding the formation of overhangs on the surface [46]. We checked that the noise generated has a correlator with the correct scaling at very long times with the desired decay exponent θ (see Appendix for details). Other popular methods to generate power-law correlated noise, like those based on Fourier filtering techniques, are infeasible for this problem, as discussed in the Appendix.

B. Ballistic deposition

We simulated ballistic deposition in the presence of long-term correlated noise by implementing the following discrete time evolution for the surface:

$$h(x, t + 1) = \max\,[h(x, t) + \eta(x, t), h(x - 1, t), h(x + 1, t)],$$

where the height $h(x, t)$ is an integer and the noise $\eta \in \{0, 1\}$ is temporally correlated as in Eq. (3) with an exponent $0 \leqslant \theta < 1/2$. Periodic boundary conditions were used and the algorithm is updated in parallel so that growth is attempted at all even (odd) sites at even (odd) time steps.

C. KPZ equation

We also carried out a numerical integration of the KPZ equation with temporally correlated noise. For reasons that will become clear later, the noise correlator (3) yields surfaces that develop a faceted pattern with an increasing local slope, $\langle|\nabla h|\rangle$, as the correlation exponent θ is increased above certain threshold. This leads to a numerical instability in finite time for any discretization of Eq. (1). To avoid this we replace the nonlinear term $\lambda(\nabla h)^2$ by an arbitrary function $\lambda f[(\nabla h)^2]$ that saturates for large values of the argument. This trick stabilizes the numerical scheme, as occurs in other growth models in which the average local slope, $\langle|\nabla h|\rangle$, becomes large [53,54]. For definiteness, the numerical results presented below correspond to the choice $f(y) = (1 - e^{-cy})/c$, where $c > 0$ is a control parameter. This is equivalent to including the infinite series of nonlinear terms $\lambda(\nabla h)^2[1 + \sum_{n=1}^{\infty}(-c)^n(\nabla h)^{2n}/(n + 1)!]$ in the evolution equation, Eq. (1), while respecting all KPZ symmetries. We have checked several choices for the control function $f(y)$, like $f(u) = u/(1 + c\,u)$, with similar results.

We discretized Eq. (1), with $f[(\nabla h)^2] = [1 - e^{-c(\nabla h)^2}]/c$ replacing $(\nabla h)^2$, with an Euler finite-differences scheme,

$$\begin{aligned} h_i(t + 1) = h_i(t) &+ \Delta t[h_{i+1}(t) + h_{i-1}(t) - 2h_i(t)] \\ &+ \Delta t\lambda\mathcal{N}_i(t) + \Delta t\,\eta_i(t), \end{aligned} \tag{4}$$

and periodic boundary conditions. The linear diffusion operator is discretized as $\nabla^2 h \to h_{i+1}(t) + h_{i-1}(t) - 2h_i(t)$ and the noise has a long-time correlator given by $\langle\eta_i(t)\eta_j(t')\rangle = 2\,\delta_{i,j}\,|t - t'|^{2\theta-1}$ with index $\theta \in [0, 1/2)$. This noise is generated as explained in Sec. II A. The nonlinear term is discretized as

$$\mathcal{N}_i(t) = (1/c)\big[1 - e^{-c[h_{i+1}(t)-h_{i-1}(t)]^2}\big],$$

where the control parameter is $c = 0.1$ in all the simulations shown here, but results are independent of this choice. We have chosen a time step $\Delta t = 10^{-3}$ for improved numerical precision, and periodic boundary conditions have been imposed in all our simulations. We have used units such that all equation parameters are unity except for the nonlinear coupling constant that is set to $\lambda = 4$, which is chosen to be large enough for the system to reach the nonlinear KPZ dominated regime early on in the simulation.

III. NUMERICAL RESULTS

In all our simulations the surface is started from a initially flat profile $h(x, 0) = 0$ and periodic boundary conditions are used. As time progresses, the surface becomes progressively rough and height fluctuations grow under the action of the random noise. Surface correlations are measured by means of height-height correlations, surface width, and the structure factor at different times in the evolution. Surface fluctuations saturate and become stationary at a characteristic time that scales with the system size, $t_\times \sim L^z$.

In Fig. 1 we plot the surface height for the ballistic deposition simulation in a system of size $L = 8192$ and correlation exponents $\theta = 0.15$ and $\theta = 0.47$. The spontaneous formation of a faceted pattern becomes apparent as the correlation index is increased. We found similar pattern formation in the numerical integration of the KPZ equation (see below).

Apart from the evident change in the visual aspect of the height profiles for $\theta > \theta_{\rm th}$, the coexistence of faceted patterns with scale invariant dynamics also leads to important effects in the scaling behavior of the surface height correlations. According to the theory of generic kinetic roughening by Ramasco *et al.* [55], scale-invariant faceted surfaces obey inherently different scaling functions (and exponents) arising from the patterned structure. Following Ramasco *et al.* [55], the most general description of the scaling properties of a growing surface is best achieved by using the structure factor $S(k, t) = \langle \widehat{h}(\mathbf{k}, t)\widehat{h}(-\mathbf{k}, t)\rangle$, where $\widehat{h}(\mathbf{k}, t) \equiv (1/L)^{d/2} \int d\mathbf{x}\, h(\mathbf{x}, t) \exp(-i\mathbf{k}\cdot\mathbf{x})$ is the Fourier transform of the surface height $h(\mathbf{x}, t)$, and $k = |\mathbf{k}|$. For kinetically roughening surfaces in $d + 1$ dimensions we expect

$$S(k, t) = k^{-(2\alpha+d)} s(kt^{1/z}), \tag{5}$$

where the most general scaling function, consistent with scale-invariant dynamics, is given by [55]

$$s(u) \sim \begin{cases} u^{2(\alpha-\alpha_s)} & \text{if } u \gg 1, \\ u^{2\alpha+d} & \text{if } u \ll 1, \end{cases} \tag{6}$$

with α being the *global* roughness exponent and α_s the so-called *spectral* roughness exponent [55]. Standard scaling corresponds to $\alpha_s = \alpha < 1$. However, other situations may be described within the generic scaling framework, including super-roughening and intrinsic anomalous scaling, depending on the values of α_s and α [55]. For faceted surfaces, the case of interest for us here, one has $\alpha_s > 1$ and $\alpha \neq \alpha_s$ so that two independent roughening exponents are actually needed to completely describe the scaling properties of the surface [55].

It is important to remark that only the structure factor $S(k, t)$ allows one to obtain the distinctively characteristic spectral roughness exponent α_s typical of faceted growing surfaces. For instance, the usual global surface width $W(L, t) = \langle [h(x, t) - \overline{h}(t)]^2\rangle^{1/2}$, where $\overline{h}(t)$ is the spatial average height at time t and the brackets $\langle \cdots \rangle$ denote average over noise, can be analytically calculated from Eqs. (5) and (6) using

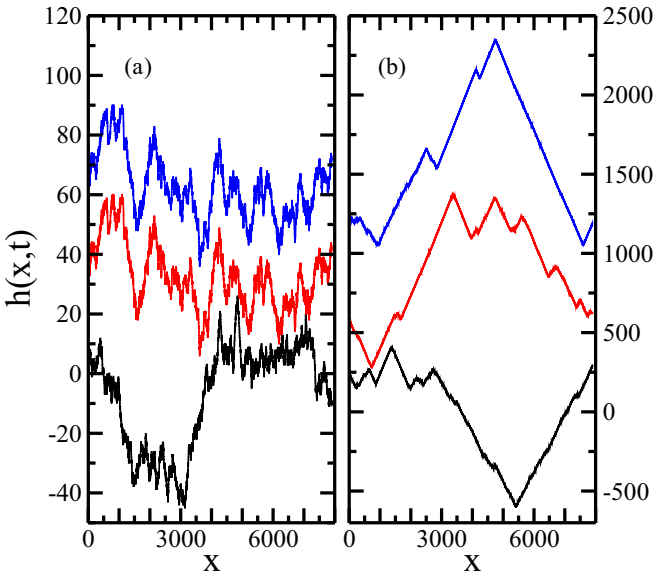

FIG. 1. Snapshots at three different times, $t_1 = 4 \times 10^4$ (black), $t_2 = 7 \times 10^4$ (red), and $t_3 = 1 \times 10^5$ (blue), of the ballistic deposition model for the noise correlator exponents $\theta = 0.15$ (a) and $\theta = 0.47$ (b), in a system of size $L = 8192$. Profiles were shifted in the vertical axis for easy view.

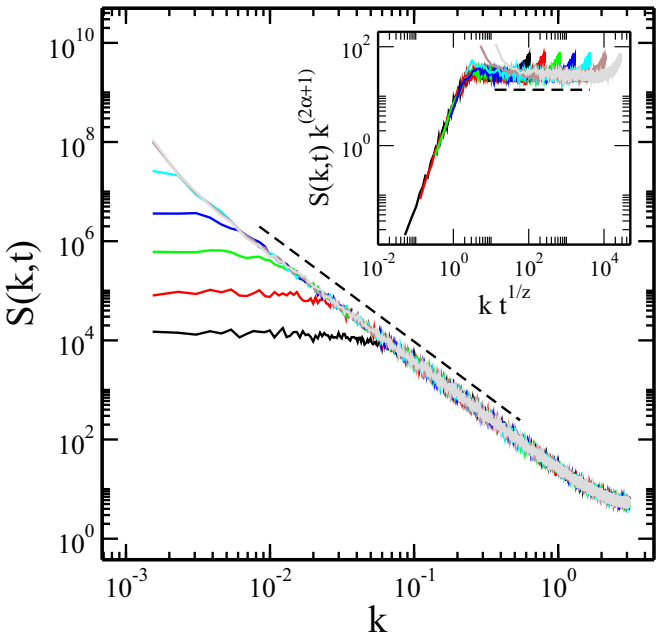

FIG. 2. Structure factor for the ballistic deposition model at different times in a system of size $L = 8192$ for $\theta = 0.15$. In the inset, we plot the collapse of spectral densities using the critical exponents $\alpha = 0.56$ and $z = 1.50$. Data were averaged over 100 independent noise realizations.

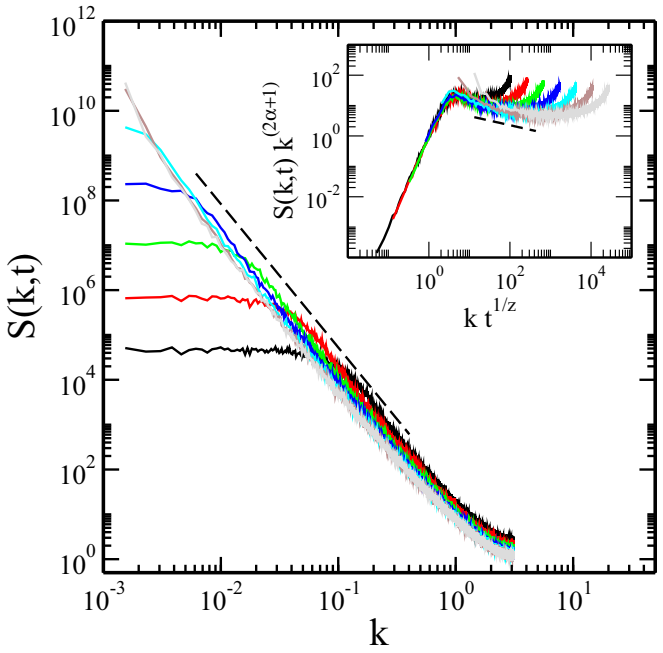

FIG. 3. Structure factor for the ballistic deposition model at different times in a system of size $L = 8192$ in the faceted face, for $\theta = 0.47$. In the inset, we plot the collapse of spectral densities using the critical exponents $\alpha = 1.02$ and $z = 1.50$. Data were averaged over 100 independent noise realizations.

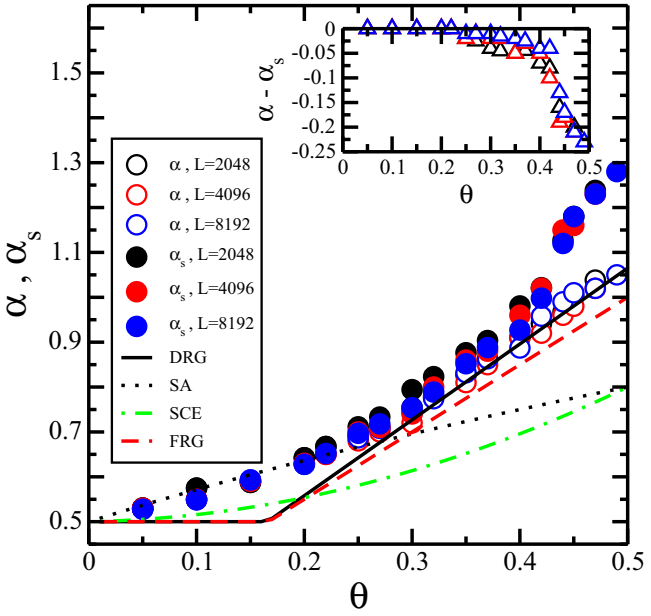

FIG. 4. Global and spectral roughness exponents as a function of the noise correlator index θ for the ballistic deposition model. For comparison, existing theoretical predictions for α of the dynamical RG treatment [30], Flory scaling approximation (SA) [56], self-consistent expansion approach (SCE) [47], and functional RG [57] approximation are plotted. The inset shows the difference $\alpha - \alpha_s$ as a function of θ showing the splitting of the exponents at $\theta_{\text{th}} \approx 0.25$.

$W^2(L,t) = \int \frac{dk}{2\pi} S(k,t)$ to obtain $W(L,t) = t^{\alpha/z}\mathcal{F}(L/t^{1/z})$, where the standard scaling function is $\mathcal{F}(u) \sim u^{\alpha}$ for $u \ll 1$ and $\mathcal{F}(u) \sim$ const for $u \gg 1$, as was shown in Ref. [55]. Hence, the anomalous spectral exponent α_s leaves no trace in the usual height-height correlation functions.

In our simulations we analyzed the structure factor $S(k,t)$ of surfaces produced with the ballistic deposition algorithm and the discretized KPZ equation for noise with correlation index θ varying in the interval $[0, 1/2)$. In Figs. 2 and 3 we plot our results for ballistic growth with correlated noise exponents $\theta = 0.15$ and $\theta = 0.47$, respectively. These θ values correspond to those plotted in Fig. 1 for easy comparison. Data collapse analysis was used to obtain the scaling behavior of $S(k,t)$ (insets of Figs. 2 and 3). For the largest system size we used, $L = 8192$, this analysis reveals that the structure factor indeed exhibits anomalous scaling, which corresponds to faceted scale-invariant surface roughening, in the case $\theta = 0.49$ with a spectral roughness exponent $\alpha_s = 1.28 \pm 0.05$ and roughness exponent $\alpha = 1.05 \pm 0.05$, while $\alpha_s = \alpha = 0.59 \pm 0.03$ (i.e., standard scaling) for $\theta = 0.15$. The dynamic exponent $z = 1.50 \pm 0.03$ remains unchanged with θ.

We have systematically analyzed the scaling behavior of the structure factor for the ballistic deposition model and the discretized KPZ equation as the correlation range of the noise, θ, is varied in the interval $[0, 1/2)$. We computed the scaling exponents α and α_s from data collapse analysis of $S(k,t)$ for system sizes $L = 2048$, 4096, and 8192. Note that large system sizes are required for the surface to develop a faceted pattern before it saturates. Our main results are summarized in Fig, 4, where the global roughness exponent α and the spectral roughness exponent α_s are plotted as a function of the noise correlation index θ for ballistic deposition growth. Similar results were obtained for the numerical integration of the KPZ equation with correlated noise (see below), demonstrating that our findings are robust within the universality class. Figure 4 clearly shows that the roughness exponents split up at $\theta_{\text{th}} = 0.25 \pm 0.03$ for the ballistic deposition model. So, below the threshold one finds standard scaling with $\alpha = \alpha_s$ and no facets. In contrast, as the noise correlation range is increased above the threshold, faceted surfaces are formed and α_s moves away from α. For the sake of comparison, Fig. 4 also shows the main theoretical approximations to KPZ with temporally correlated noise. We can see that, while the global roughness exponent is nicely predicted by the dynamic RG calculations of Medina *et al.* [30] above the threshold, it fails to describe the correlation effects below θ_{th}. Obviously, no present theory is capable of predicting the existence of facets and the associated spectral roughness exponent as the noise correlation range is increased.

We have also integrated the KPZ equation with power-law temporally correlated noise by means of the numerical scheme described by Eq. (4) in systems of size $L = 1024$, 2048, and 4096 for times long enough to reach saturation of the surface fluctuations. Data for the structure factor $S(k,t)$ were collapsed and fitted according to the generic scaling behavior given by Eqs. (5) and (6) for values of the noise correlator index in the interval $\theta \in [0, 0.5)$. In Fig. 5 we plot typical profiles of the time evolution for a realization of the KPZ equation for noise correlator exponents $\theta = 0.15$ and

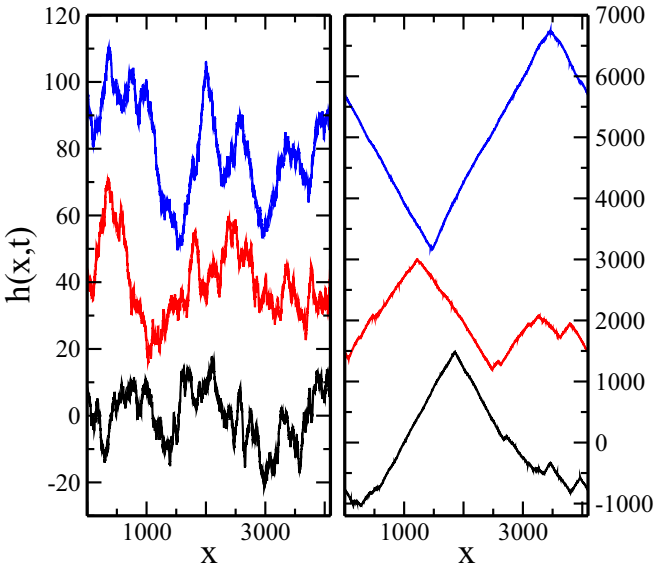

FIG. 5. Snapshots at three different times, 4×10^4 (black), 7×10^4 (red), and 1×10^5 (blue), for the KPZ integration and the noise correlator exponents $\theta = 0.15$ (a) and $\theta = 0.47$ (b), in a system of size $L = 4096$. Profiles were shifted in the vertical axis for easy view.

$\theta = 0.47$, showing the formation of the faceted pattern for higher noise correlations. In Fig. 6 we plot a summary of our numerical results for KPZ with correlated noise showing that the splitting of the global and spectral exponents takes place around $\theta_{\text{th}} = 0.23 \pm 0.03$.

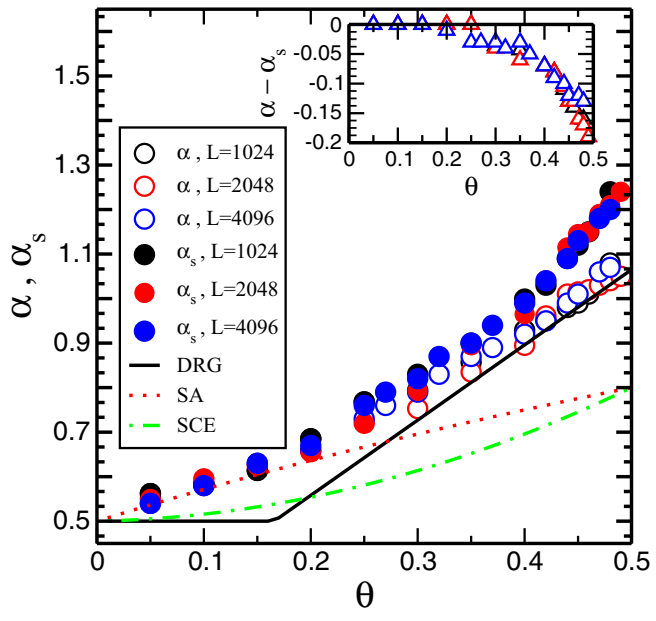

FIG. 6. Global and spectral roughness exponents as a function of the noise correlator index θ for the numerical integration of KPZ. For comparison, the existing theoretical predictions for α of the RG treatment [30], Flory scaling approximation (SA) [56], and self-consistent expansion approach (SCE) [47] are plotted. The inset shows the difference $\alpha - \alpha_s$ as a function of θ showing the splitting of the exponents at $\theta_{\text{th}} \approx 0.23$

IV. DISCUSSION

While we lack of a complete theory to explain the numerical findings reported above, we can put forward some arguments to rationalize the emergence of the faceted patterns and the associated anomalous scaling.

Let us start by considering the limit case of KPZ dynamics with the noise at site each site $\mathbf{x}$ fixed at all times, but uncorrelated from site to site—namely, the problem of KPZ with columnar noise:

$$\partial_t h(\mathbf{x}, t) = \nabla^2 h + \lambda(\nabla h)^2 + \eta(\mathbf{x}), \tag{7}$$

where $\eta(\mathbf{x})$ is a spatially uncorrelated noise

$$\langle \eta(\mathbf{x})\eta(\mathbf{x}')\rangle = \delta(\mathbf{x} - \mathbf{x}').$$

This problem corresponds to the limit $\theta = 1/2$ of the correlated noise case in Eq. (3). It is well known [58] that the *columnar* KPZ equation (7) exhibits facet formation arising from the exponential localization of the field $\phi(\mathbf{x}, t) \equiv \exp h(\mathbf{x}, t)$ around some random centers $\mathbf{x}_c$ [59]. The auxiliary ϕ can be interpreted as the probability density of particles diffusing in a random potential $\eta(\mathbf{x})$:

$$\partial_t \phi = \nabla^2 \phi + \eta(\mathbf{x})\phi(\mathbf{x}, t). \tag{8}$$

The multiplicative-noise term in Eq. (8) leads to sharply localized solutions around random localization centers [59]. The stochastic field ϕ has an exponential profile, $\sim \exp(-|\mathbf{x} - \mathbf{x}_c|/\xi)$, around any typical center $\mathbf{x}_c$ with a certain localization extent ξ. The solutions of Eq. (8) are, therefore, a superposition of these exponentially localized functions. In turn, this leads to a surface h formed by facets with their cusps at the localization centers, $h \sim \ln \phi \sim \pm|\mathbf{x} - \mathbf{x}_c|/\xi$, as shown by Szendro *et al.* [58]. There, the reported values of the global and spectral roughness exponents were $\alpha = 1.07 \pm 0.05$ and $\alpha_s = 1.5 \pm 0.05$, respectively, in $d = 1$.

Our numerical results indicate that the mechanism for the formation of facets based on localization can explain the formation of facets for $\theta < 1/2$. We find that anomalous scaling, $\alpha_s \neq \alpha$, occurs for $\theta > 1/4$. Remarkably, the value $\theta = 1/4$ was already shown to play a special role in the perturbative RG approximation of Medina *et al.* [30], as the point at which the renormalized noise amplitude $D^*(\omega)$ has a singular correction at leading ω order. Further singularities appear at larger values of θ making the RG treatment ill-constructed. Note that the functional RG approximation developed by Fedorenko [57] apparently solved these technical difficulties because no singularities appear in the FRG treatment. However, neither dynamical RG nor functional RG approximations are able to describe the appearance of a new exponent $\alpha_s \neq \alpha$ or are able to accommodate the existence of a faceted phase as θ increases. Given these results, it becomes clear that a generalization of the RG theory would be required to describe the generic scaling form (6) of the spectral function. Such a generalization should be able not only to fix the nonphysical singularities but it would also provide a coherent mathematical picture of anomalous kinetic roughening as a whole.

ACKNOWLEDGMENTS

J.M.L. thanks D. Pazó for discussions and a critical reading of the manuscript. This work has been partially supported by the Program for Scientific Cooperation "I-COOP+" from Consejo Superior de Investigaciones Científicas (Spain) through Project No. COOPA20187. A.A. is grateful for the financial support from Programa de Pasantías de la Universidad de Cantabria in 2017 and 2018 (Projects No. 70-ZCE3-226.90 and No. 62-VCES-648), and CONICET (Argentina) for a Doctoral Fellowship. J.M.L is supported by Dirección General de Investigación Científica y Técnica, Ministerio de Economía, Industria y Competitividad (Spain), through Project No. FIS2016-74957-P.

APPENDIX: GENERATION OF LONG-TIME CORRELATED NOISE

We needed to generate a spatially uncorrelated time series with a power spectrum that exhibits excellent scaling at low frequencies so that, at leading order, $\langle|\hat{\eta}(x,\omega)|^2\rangle \sim \omega^{-2\theta}$ for $\omega \to 0$ at every lattice site x. In this way we have time correlations in the noise that extend for time differences $|t-t'|$ much larger than surface saturation time. For this purpose we used Mandelbrot's fast fractional Gaussian noise generator [51,52]. Details can be found in the original papers but here we want to give a brief description of the algorithm and test the quality of the noise correlations generated by this procedure. Although one of the most popular methods for generating sequences of random numbers with power-law correlations is the Fourier filtering technique [60,61], that method requires generating the complete temporal sequence of random numbers for each site at the beginning of the simulation and keep it in the computer memory, making it useless for the very long random sequences we need here.

The construction of the series is carried out in the following way: the term of low frequency comes from the weighted sum of N terms of Markov-Gauss type, and the mathematical expression corresponds to

$$Z(t) = \sum_{n=1}^{N} W_n X(t, r_n|MG), \tag{A1}$$

where W_n are weight functions for different characteristic frequencies and the terms $X(t, r_n|MG)$ are Markov-Gaussian processes with unit variance and covariance $r_n = e^{-B^{-n}}$, the parameter B being a base greater than the unit conveniently chosen. The weight function has the following form:

$$W_n^2 = \frac{2\theta(1/2+\theta)[B^{(1/2-\theta)} - B^{(1/2+\theta)}]}{\Gamma(2-2\theta)} B^{2(\theta-1/2)n},$$

where Γ is the complete gamma function. The number of terms $N(T)$ to be added in the sum (A1) increases with the the correlation time T and is given by the following expression:

$$N(T) = \frac{\log(QT)}{\log(B)},$$

where Q is *quality factor* and may be increased to achieve the desired power-law tail exponent θ with higher precision at low frequencies. The increase in the number of terms N to be added leads to a better approximation at the expense of higher computational cost. The Markov-Gaussian processes are determined according to the following sequence: for the first temporal step, all the terms of the summation of the

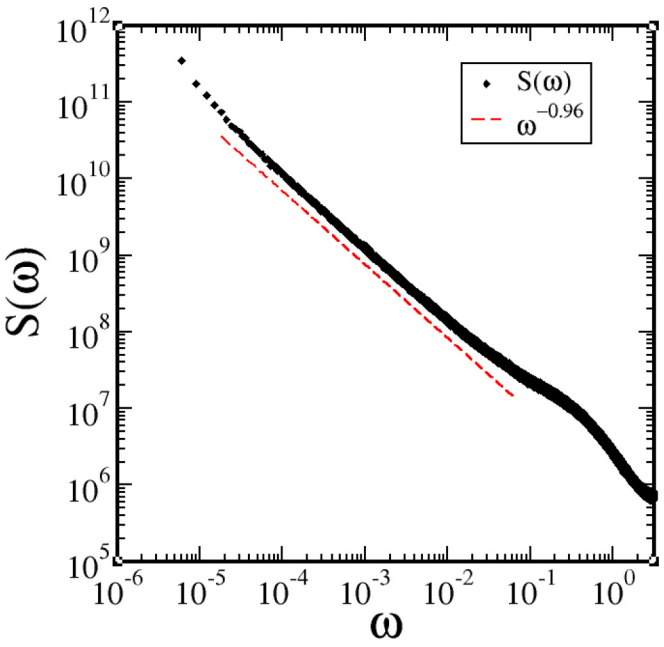

FIG. 7. Power spectrum of a correlated noise series with exponent $\theta = 0.48$ and the curve $\sim\omega^{-2\theta}$ describing the low-frequency scaling. Data were averaged over 10^3 independent realizations of the noise.

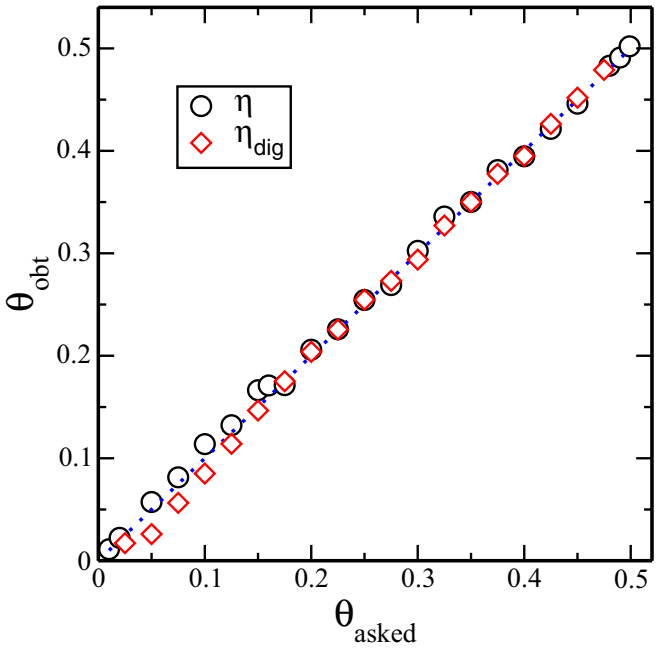

FIG. 8. Comparison of the asked correlation exponent (θ_{asked}) with the one actually obtained (θ_{obt}) with Mandelbrot's algorithm, including the *digitalized* noise used in the ballistic deposition simulations.

expression (A1) are Gaussian white noises ξ_n:

$$X(1, r_n|MG) = \xi_n(1).$$

Then, for the second term onward, a recurrence rule is used to obtain the noise series as follows:

$$X(t, r_n|MG) = r_n X(t-1, r_n|MG) + \sqrt{1-r_n^2}\,\xi_n(t),$$

where $\xi_n(t)$ is a white noise. This computations require keeping in the computer memory only the latest noise value $X(t-1, r_n|MG)$ and the generation of N uncorrelated Gaussian numbers ξ_n at every time step.

The correct implementation of the long-termed correlation requires testing of the base parameter B and quality factor Q to be used. For generating a correlated noise time series of length $T = 2^{21}$ we used $B = 3$ and $Q = 100$. These parameters allowed us to obtain a noise with a power spectrum displaying a long tail in the form of a power-law decay with the desired exponent for all $\theta \leqslant 0.49$. As an example, in Fig. 7 we show the power spectrum of the correlated noise for the demanding case of $\theta = 0.48$. It can be seen that the tail behaves satisfactorily for low frequencies, as required.

In Fig. 8 we show a comparison of the asked correlation exponent, θ_{asked}, with the one actually obtained, θ_{obt}, with Mandelbrot's algorithm, including the noise *digitization* used in the ballistic deposition simulations.

[1] A.-L. Barabási and H. E. Stanley, *Fractal Concepts in Surface Growth* (Cambridge University Press, Cambridge, 1995), p. 386.
[2] J. Krug, Adv. Phys. **46**, 139 (1997).
[3] M. J. Alava, P. K. V. V. Nukala, and S. Zapperi, Adv. Phys. **55**, 349 (2006).
[4] M. Alava, M. Dubé, and M. Rost, Adv. Phys. **53**, 83 (2004).
[5] M. Kardar, Phys. Rep. **301**, 85 (1998).
[6] T. Halpin-Healy and Y. C. Zhang, Phys. Rep. **254**, 215 (1995).
[7] D. Pazó, J. M. López, and A. Politi, Phys. Rev. E **87**, 062909 (2013).
[8] D. Pazó, J. M. López, and A. Politi, Phys. Rev. Lett. **117**, 034101 (2016).
[9] A. Pikovsky and A. Politi, Nonlinearity **11**, 1049 (1998).
[10] D. Pazó, J. M. López, R. Gallego, and M. A. Rodríguez, Chaos **24**, 043115 (2014).
[11] D. Pazó, I. G. Szendro, J. M. López, and M. A. Rodríguez, Phys. Rev. E **78**, 016209 (2008).
[12] A. Pikovsky and A. Politi, Phys. Rev. E **63**, 036207 (2001).
[13] I. G. Szendro, D. Pazó, M. A. Rodríguez, and J. M. López, Phys. Rev. E **76**, 025202(R) (2007).
[14] D. Pazó, J. M. López, and M. A. Rodríguez, Phys. Rev. E **79**, 036202 (2009).
[15] H. G. E. Hentschel, J. Phys. A: Math. Gen. **27**, 2269 (1994).
[16] M. Kardar, G. Parisi, and Y.-C. Zhang, Phys. Rev. Lett. **56**, 889 (1986).
[17] J. M. Kim and J. M. Kosterlitz, Phys. Rev. Lett. **62**, 2289 (1989).
[18] J. M. Kim, J. M. Kosterlitz, and T. Ala-Nissila, J. Phys. A: Math. Gen. **24**, 5569 (1991).
[19] K. Moser, J. Kertész, and D. E. Wolf, Physica A **178**, 215 (1991).
[20] T. Ala-Nissila, T. Hjelt, and J. M. Kosterlitz, Europhys. Lett. **19**, 1 (1992).
[21] T. Ala-Nissila, T. Hjelt, J. M. Kosterlitz, and O. Venäläinen, J. Stat. Phys. **72**, 207 (1993).
[22] B. M. Forrest and L.-H. Tang, Phys. Rev. Lett. **64**, 1405 (1990).
[23] V. G. Miranda and F. D. A. Aarão Reis, Phys. Rev. E **77**, 031134 (2008).
[24] S. G. Alves, T. J. Oliveira, and S. C. Ferreira, Phys. Rev. E **90**, 020103(R) (2014).
[25] S. G. Alves and S. C. Ferreira, Phys. Rev. E **93**, 052131 (2016).
[26] F. Colaiori and M. A. Moore, Phys. Rev. Lett. **86**, 3946 (2001).
[27] L. Canet, H. Chaté, B. Delamotte, and N. Wschebor, Phys. Rev. Lett. **104**, 150601 (2010).
[28] M. Schwartz and S. F. Edwards, Europhys. Lett. **20**, 301 (1992).
[29] H. C. Fogedby, Phys. Rev. E **73**, 031104 (2006).
[30] E. Medina, T. Hwa, M. Kardar, and Y.-C. Zhang, Phys. Rev. A **39**, 3053 (1989).
[31] T. Halpin-Healy, Phys. Rev. Lett. **62**, 442 (1989).
[32] P. Meakin and R. Jullien, Europhys. Lett. **9**, 71 (1989).
[33] Y.-C. Zhang, Phys. Rev. B **42**, 4897 (1990).
[34] A. Margolina and H. Warriner, J. Stat. Phys. **60**, 809 (1990).
[35] J. G. Amar, P.-M. Lam, and F. Family, Phys. Rev. A **43**, 4548 (1991).
[36] C.-K. Peng, S. Havlin, M. Schwartz, and H. E. Stanley, Phys. Rev. A **44**, R2239(R) (1991).
[37] M. Wu, K. Y. R. Billah, and M. Shinozuka, Phys. Rev. E **51**, 995 (1995).
[38] N.-N. Pang, Y.-K. Yu, and T. Halpin-Healy, Phys. Rev. E **52**, 3224 (1995).
[39] H. Jeong, B. Kahng, and D. Kim, Phys. Rev. E **52**, R1292 (1995).
[40] M. S. Li, Phys. Rev. E **55**, 1178 (1997).
[41] H. Janssen, U. Täuber, and E. Frey, Eur. Phys. J. B **9**, 491 (1999).
[42] M.-P. Kuittu, M. Haataja, and T. Ala-Nissila, Phys. Rev. E **59**, 2677 (1999).
[43] E. Katzav and M. Schwartz, Phys. Rev. E **60**, 5677 (1999).
[44] M. K. Verma, Physica A **277**, 359 (2000).
[45] T. Kloss, L. Canet, B. Delamotte, and N. Wschebor, Phys. Rev. E **89**, 022108 (2014).
[46] C.-H. Lam, L. M. Sander, and D. E. Wolf, Phys. Rev. A **46**, R6128 (1992).
[47] E. Katzav and M. Schwartz, Phys. Rev. E **70**, 011601 (2004).
[48] P. Strack, Phys. Rev. E **91**, 032131 (2015).
[49] T. Song and H. Xia, J. Stat. Mech.: Theory Exp. (2016) 113206.
[50] M. Romero-Bastida, D. Pazó, J. M. López, and M. A. Rodríguez, Phys. Rev. E **82**, 036205 (2010).
[51] B. B. Mandelbrot and J. R. Wallis, Water Resour. Res. **5**, 228 (1969).

[52] B. B. Mandelbrot, Water Resour. Res. **7**, 543 (1971).
[53] C. Dasgupta, S. Das Sarma, and J. M. Kim, Phys. Rev. E **54**, R4552(R) (1996).
[54] C. Dasgupta, J. M. Kim, M. Dutta, and S. Das Sarma, Phys. Rev. E **55**, 2235 (1997).
[55] J. J. Ramasco, J. M. López, and M. A. Rodríguez, Phys. Rev. Lett. **84**, 2199 (2000).
[56] Hanfei and B. Ma, Phys. Rev. E **47**, 3738 (1993).
[57] A. A. Fedorenko, Phys. Rev. B **77**, 094203 (2008).
[58] I. G. Szendro, J. M. López, and M. A. Rodríguez, Phys. Rev. E **76**, 011603 (2007).
[59] T. Nattermann and W. Renz, Phys. Rev. A **40**, 4675 (1989).
[60] *The Science of Fractal Image*, edited by H.-O. Peitgen and D. Saupe (Springer-Verlag, New York, 1988).
[61] H. A. Makse, S. Havlin, M. Schwartz, and H. E. Stanley, Phys. Rev. E **53**, 5445 (1996).